

Planet Migration in Planetesimal Disks

Harold F. Levison

Southwest Research Institute, Boulder

Alessandro Morbidelli

Observatoire de la Côte d'Azur

Rodney Gomes

Observatório Nacional, Rio de Janeiro

Dana Backman

USRA and SETI Institute, Moffett Field

Planets embedded in a planetesimal disk will migrate as a result of angular momentum and energy conservation as the planets scatter the planetesimals that they encounter. A surprising variety of interesting and complex dynamics can arise from this apparently simple process. In this chapter, we review the basic characteristics of planetesimal-driven migration. We discuss how the structure of a planetary system controls migration. We describe how this type of migration can cause planetary systems to become dynamically unstable and how a massive planetesimal disk can save planets from being ejected from the planetary system during this instability. We examine how the solar system's small-body reservoirs, particularly the Kuiper belt and Jupiter's Trojan asteroids, constrain what happened here. We also review a new model for the early dynamical evolution of the outer solar system that quantitatively reproduces much of what we see. And finally, we briefly discuss how planetesimal-driven migration could have affected some of the extrasolar systems that have recently been discovered.

1. INTRODUCTION

Our understanding of the origin and evolution of planets has drastically transformed in the last decade. Perhaps the most fundamental change was the realization that planets, in general, may not have formed in the orbits in which we see them. Indeed, planets may have migrated huge distances after they were born, as many of the extrasolar planetary systems show (*Moorhead and Adams, 2005; Papaloizou and Terquem, 2006*).

There are three main dynamical mechanisms that can cause such a wholesale evolution in planetary orbits. First, at early times when the natal protoplanetary gas disk is still in existence, gravitational interactions between the disk and a planet could cause a significant amount of orbital evolution (see chapter by Papaloizou et al. for a discussion). Second, after the gas disk is gone, if there still is a significant number of planetesimals in the system, the planets can migrate as a result of gravitational encounters with these objects. In particular, if a planet is immersed in a sea of small bodies, it will recoil every time it gravitationally scatters one of these objects. In general, since the small objects can

come in from any direction, this will force the planets to undergo a small random walk in semimajor axis. However, since the sinks for these objects, for example, ejection from the system or encountering a neighboring planet, tend to lie on one side of the planet in question or another, there will be a net flux of material inward or outward. The planet must move in the opposite direction in order to conserve energy and angular momentum. In the absence of strong gravitational perturbations from other planets, the semimajor axis of planet in question will smoothly change with time. In the remainder of this chapter, we refer to this type of migration as *simple* migration. Third, planetary systems can suffer a dynamical instability (*Levison et al., 1998*) that can lead to a short but violent period of orbital evolution during which the planetary eccentricities are increased to large values (*Rasio and Ford, 1996*). If the instability can be damped by some process (like dynamical friction with a disk), the planets can once again evolve onto nearly circular orbits, but in very different locations from where they formed. It has been suggested that this kind of instability occurred in the outer parts of our planetary system (*Thommes et al., 1999; Levison et al., 2001; Tsiganis et al., 2005*).

The primary foci of this chapter are the second and the third mechanisms described above; namely migration in planetesimal disks. Although we claimed at the opening of this chapter that the role that planetesimal-driven migration played in the evolution of planetary systems was only acknowledged within the last decade, the idea itself is more than 20 years old. The first discussion of this process was presented by *Fernández and Ip* (1984). Their paper describes the response of Jupiter, Saturn, Uranus, and Neptune to a remnant disk of planetesimals. Although many of the details have changed as our ability to perform orbital integrations has improved, these authors found the basic result that is still held true today.

The importance of the work by Fernández and Ip was not really appreciated until the discovery of the Kuiper belt nearly a decade later, with its numerous objects on eccentric orbits in mean-motion resonances with Neptune. *Malhotra* (1993, 1995) first showed that these orbits could be the natural result of Neptune’s outward migration and concluded that Neptune must have migrated about 7 AU in order to explain the eccentricities that we see (cf. section 3).

Much work as been done on this topic since Fernández and Ip’s and Malhotra’s groundbreaking papers. This literature is the topic of the remainder of the chapter, although it should be noted that this chapter is intended more as discussion of the current state-of-the-art than a review paper. In section 2 and section 3 we describe some of the basic physics that govern planet migration and resonant capture, respectively. In section 4, we examine simple planetesimal-driven migration in the solar system. In section 5 we look at how instabilities in the orbits of the planets, coupled with gravitational interactions with a massive planetesimal disk, could lead to significant changes in the orbits of the planets. We review a new model for the early dynamical evolution of the giant planets of the solar system in section 6, and planetesimal-driven migration in extrasolar systems in section 7. In section 8 we discuss some caveats and limitations of the N-body simulations on which most of the content of this chapter is based. We present our concluding remarks in section 9.

2. BASIC PRINCIPLES OF SIMPLE MIGRATION

The migration history for each individual planet is complicated because it is dependent on the details of how angular momentum flows through the system, namely on the distribution and the evolution of the mass and the angular momentum of the planet-crossing objects. These quantities, in turn, are determined by the sources and sinks for these particles. As a result, attempts to develop analytic theories for migration have studied very simple systems consisting of a single planet in a dynamically cold disk (*Murray et al.*, 1998; *Ida et al.*, 2000, hereafter *IBLT00*). So, the goal of this section is not to develop a comprehensive analytical model, but to develop a toy model to help cultivate a quali-

tative understanding of some of the important physical processes involved. Much of what we present is based on the work in *Gomes et al.* (2004, hereafter *GML04*). We start with a very simple model.

2.1. A Simple Model

IBLT00 shows that the rate of change of a planet’s semi-major axis, a , is

$$\frac{da}{dt} = -\frac{2}{M_p} \sqrt{a} \dot{H}_x \quad (1)$$

where M_p is the mass of the planet, and \dot{H}_x is the rate of transfer of angular momentum from the planetesimals to the planet. This equation assumes that the eccentricity of the planet is small and $G \equiv 1$. Using the particle-in-a-box approximation, it is possible to show that $\dot{H}_x = \epsilon \bar{k} M(t) a^{-1}$, where ϵ is a quantity that contains fundamental constants and information about the geometry of the planet-encountering region, $M(t)$ is the total mass in planet-encountering orbits, and \bar{k} is the average change of angular momentum per encounter, per unit mass planetesimal. Thus

$$\frac{da}{dt} = -2\epsilon \bar{k} \frac{M(t)}{M_p} \frac{1}{\sqrt{a}} \quad (2)$$

The evolution of $M(t)$ can be approximated by the equation

$$\dot{M}(t) = -M(t)/\tau + 2\pi a |\dot{\Sigma}(a)| \quad (3)$$

where the first term in the r.h.s. represents the decay of the planetesimal population due to the planetesimal’s finite dynamical lifetime, and the second term stands for the planetesimals that, because of the change in the planet’s position, enter the region where they can be scattered by the planet for the first time. In equation (3) $\Sigma(a)$ is the surface density of the “virgin” (i.e., not yet scattered) planetesimal disk at heliocentric distance a . Substituting equation (2) into equation (3) we get

$$\dot{M}(t) = (-\tau^{-1} + 4\pi \epsilon |\bar{k}| \sqrt{a} \Sigma(a) / M_p) M(t) \quad (4)$$

Let’s assume for simplicity that the term $\alpha \equiv -\tau^{-1} + 4\pi \epsilon |\bar{k}| \sqrt{a} \Sigma(a) / M_p$ does not significantly change with time — an approximation that is clearly not true, but it allows us to get the essence of the planet’s behavior. Under this assumption, equation (4) becomes an exponential equation, which is solvable and thus will allow us to get some insight into how the planet migrates.

If α is negative, then $M(t)$ decays exponentially to 0 and the planet (from equation (1)) stops migrating. In this case, the loss of planetesimals due to their finite dynamical life-

time is not compensated by the acquisition of new planetesimals into the scattering region. Therefore, the planet runs “out of fuel.” *GML04* called this migration mode *damped migration*. Conversely, if α is positive, $M(t)$ grows exponentially and the planet’s migration accelerates. In this case the acquisition of new planetesimals due to the migration exceeds the losses, and the migration is sustained. Thus, we will call this migration mode *sustained migration*.

2.2. The Direction of Migration

One of the limitations of the above description is that it does not contain any direct information about the direction of migration. This information is hidden in \bar{k} . Recall that the migration process is driven by gravitational encounters between planets and disk particles. To zeroth order, during an encounter the two objects are in a Kepler orbit about one another. Since the energy of this orbit must be conserved, all the encounter can do is rotate the relative velocity vector between the pair. Thus, the consequences of such an encounter can be effectively computed in most of the cases using an impulse approximation (*Opik, 1976*; also see *IBLT00*). Using this approach, it is easy to compute that on average (i.e., averaged on all impact parameters and relative orientations) the planetesimals that cause a planet to move outward are those whose z -component of the angular momentum $H = \sqrt{a(1-e^2)} \cos i$ is larger than that of the planet (H_p). The opposite is true for the planetesimals with $H < H_p$ (*Valsecchi and Manara, 1997*). In these formulae, e and i are the semimajor axis, eccentricity, and inclination of the planetesimal. Thus, \bar{k} is a function of the angular momentum distribution of objects on planet-encountering orbits, and it is positive if more material has $H > H_p$, zero if the average H is the same as H_p , and negative otherwise.

The main physical effect that was not included in the derivation of equation (4) was the influence that the particles both entering and leaving the planet-encountering region can have on \bar{k} . For a single planet in a disk, there are two main sinks for the particles. Particles can hit the planet (this is the only sink that *IBLT00* considered). Since the chance of hitting the planet is roughly independent of the sign of $H - H_p$, in general this sink will not effect \bar{k} and thus it is migration neutral. In addition, a planet can eject particles. These particles remove energy and thus the planet must move inward in response. The ability of a planet to eject particles depends on the dynamical excitation of the disk. We characterize the latter by the parameter $v' \equiv v_{\text{enc}}/v_c$, where v_{enc} is the typical encounter velocity of disk particles with the planet, and v_c is the planet’s circular velocity. No matter how massive a planet is, it cannot eject a particle if the particle’s $v' < v^*$, where $v^* = \sqrt{2} - 1 \approx 0.4$. However, v' is only conserved if the planet is on a circular orbit. In cases where that is not true, ejection can occur even if the disk is initially cold.

Multiple planet systems allow for another sink — particles can be transferred from one planet to another. The

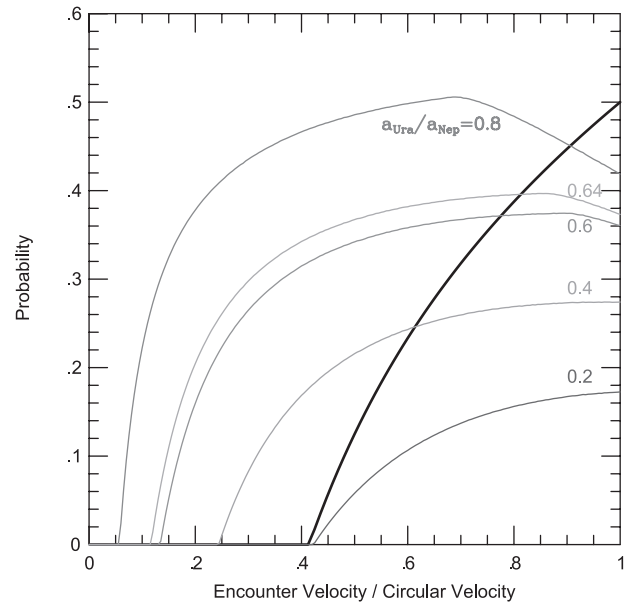


Fig. 1. The probability of a particular dynamical outcome resulting from an encounter between a small body and Neptune, as a function of the encounter velocity. The thick black curve shows the probability of ejection as determined by equation (5). The gray curves show the probability that the encounter will lead to the object being scattered onto a bound “Uranus-crossing” orbit for different semimajor axes of Uranus. These curves were determined from simple analytic arguments or simple numerical experiments (see text).

best example is provided by the solar system’s four giant planets. Numerical experiments show that in the interaction with a disk of planetesimals Jupiter moves inward, but the other three giants move outward (*Fernández and Ip, 1984*; *Hahn and Malhotra, 1999*; *Gomes et al., 2004*). We can illustrate why Neptune moves outward with the following hand-waving argument. An object’s velocity in an inertial frame is $\vec{v} = \vec{v}_c + \vec{v}_{\text{enc}}$. Assuming that after the encounter \vec{v}_{enc} is pointing in a random direction, the probability of ejection is

$$P_{\text{eject}} = \left(\frac{v'^2 + 2v' - 1}{4v'} \right) \quad (5)$$

(the thick black curve in Fig. 1).

The probability that an object is transferred to Uranus (i.e., acquires an orbit with perihelion distance $q < a_{\text{Ura}}$) depends on v' and on the ratio of Uranus’ semimajor axis to that of Neptune ($a_{\text{Ura}}/a_{\text{Nep}}$). It can be evaluated using a Monte Carlo method, if the assumption used to derive equation (5) is again made. The gray curves in Fig. 1 show the results for five different values of $a_{\text{Ura}}/a_{\text{Nep}}$. Currently $a_{\text{Ura}}/a_{\text{Nep}} = 0.64$. Figure 1 shows that if $a_{\text{Ura}}/a_{\text{Nep}} \geq 0.3$ and $v' \leq$

0.5, Neptune is more likely to transfer objects to Uranus than to eject them. This explains why this planet moves outward.

So far we have considered only the planetesimal sinks in the planet-migration process. In addition to these, there are two ways in which new particles can be added to the planet-crossing population. The first of these is actually a source/sink pair caused by the migration process itself. As the planet moves, so does the planet-encountering region and thus some particles leave this region while new particles enter it. If the planet is moving outward, the particles that leave have $H < H_p$, while those that enter have $H > H_p$. The opposite is true if the planet is moving inward. Thus, this process tends to support any migration that was started by another mechanism.

Resonances with the planet are another source for particles. Objects originally in the chaotic regions of these resonances can have their eccentricities pumped until their orbits start to encounter the planet (cf. *Duncan et al.*, 1995). The effect that this source has on \bar{k} depends on the planetesimal surface density profile and on the strength of the resonances.

To summarize, the actual migration behavior of planets depends on a competition between the various sources and sinks. If the material in the planet-encountering region is removed faster than it is replenished, the planet's migration rate will decay to zero. We call this behavior *damped* migration. If the planet-encountering region is replenished faster than it is depleted, the migration is said to be *sustained*. Sustained migration is divided into two types. If the migration is nourished by particles being fed into the planet-encountering region by the migration itself and the sinks do not require the presence of other planets, we refer to it as *runaway* migration. If other planets are required, we name the migration mode *forced* migration.

3. RESONANT CAPTURE DURING PLANET MIGRATION

One consequence of a planet's orbital migration is that the mean-motion resonances (MMRs) with the planet also move. During this process, disk planetesimals that are "swept" by a MMR can be captured in it. Resonance capture is a complicated process and an active subject of research in the field of nonlinear dynamics (see, e.g., *Wiggins*, 1991; *Neishtadt*, 1975, 1987, 1997; *Henrard*, 1982; *Malhotra*, 1993, 1995). The evolution of a particle interacting with a moving resonance depends sensitively on initial conditions, the nature of the resonance, the rate of evolution due to dissipative effects, etc. A model that has been studied in detail is that of a single resonance in the so-called *adiabatic approximation*. In the framework considered in this chapter, this model would correspond to a single planet on a circular orbit, migrating slowly and monotonically. The adiabatic condition is met if the time required for a resonance to move by a heliocentric distance range comparable to the resonance width is much longer than the libration

timescale inside the resonance (which itself is much longer than the orbital timescale). In this case, the probability of resonance capture has been calculated semi-analytically (*Henrard and Lemaître*, 1983; *Borderies and Goldreich*, 1984).

In essence, resonance capture can occur only in exterior MMRs (which for the resonance called the "j:j+k MMR" implies $k > 0$) if the planet is moving outward, and in interior MMRs ($k < 0$) if the planet is moving inward (*Henrard and Lemaître*, 1983; *Neishtadt*, 1987; *Tsiganis et al.*, 2005). However, if the particle is swept in the correct direction, capture into the resonance is not guaranteed. For instance, in the adiabatic approximation, capture into the 2:3 MMR with Neptune (where many Kuiper belt objects are seen, including Pluto) is certain only if Neptune is migrating outward and the initial eccentricity of the particle is less than ~ 0.03 . The capture probability decreases monotonically (but not linearly!) for higher initial eccentricities: It is less than 10% for $e > 0.15$.

If the object is captured into the resonance, it then moves with the resonance as the planets continues in its migration. During this evolution, the eccentricity of the object increases monotonically at a rate determined by the migration rate of the planet, which gives the relationship (*Malhotra*, 1995)

$$e_{\text{final}}^2 = e_{\text{initial}}^2 + \frac{j}{j+k} \ln \frac{a_{\text{p,final}}}{a_{\text{p,initial}}} \quad (6)$$

where $a_{\text{p,initial}}$ is the semimajor axis of the planet when the body enters into resonance, e_{initial} is the eccentricity of the body at that time, $a_{\text{p,final}}$ is the semimajor axis of the planet at the time of consideration, and e_{final} is the eccentricity of the object at the same instant.

Resonances, however, are not stable at all eccentricities. If the eccentricity is large enough, the resonance cannot protect the objects from close encounters with the planet. Thus, in this picture (see *Malhotra*, 1995), as the planet migrates, planetesimals are captured into MMRs, move together with the resonances while growing their orbital eccentricities until they reach the instability limit, and start to be scattered by the planet. The resonant population remains in roughly a steady state as long as the resonance remains in the disk, because new objects enter into the resonance while large eccentricity objects leave it. If the resonance passes beyond the edge of the disk, it is no longer refilled with new objects. The resonant population decays as the resonance moves away from the edge, while the minimum eccentricity of the resonant population grows, so that the low-eccentricity portion of the resonance becomes empty.

The formula in equation (6) is useful to deduce some properties of the migration. For instance, if a resonance is populated with objects up to an eccentricity equal to e_{max} (and the latter is smaller than the threshold value for instability), it means that the planet migrated a distance $\delta a_p = \exp\{[(j+k)/j]e_{\text{max}}^2\}$. *Malhotra* (1995), observing that the eccentricity of Kuiper belt objects in the 2:3 MMR is smaller

than 0.32, deduced that Neptune migrated at least 7 AU (i.e., it formed at a ≤ 23 AU).

Unfortunately, reality is not as simple as the adiabatic model predicts. If the resonance is surrounded by a chaotic layer, as it is the case if the planet's eccentricity is not zero or the inclination of the particle is large, the computation of the capture probability with semi-analytic techniques is essentially impossible, because it depends also on the diffusion speed inside the chaotic layer (Henrard and Morbidelli, 1993). Numerical simulations of migration of Neptune in more realistic models of the planetary system show that the capture probability is much less sensitive on the particles' orbital eccentricity than the adiabatic theory predicts, and resonance capture is quite likely also at large eccentricity (Chiang et al., 2003; Gomes, 2003; Hahn and Malhotra, 2005).

Another difference between reality and the adiabatic model concerns the eccentricity growth of resonant objects during the migration. While in the adiabatic model the eccentricity grows monotonically, in reality there can be secular terms forcing large-amplitude oscillations of the eccentricity in resonant objects. For example, Levison and Morbidelli (2003) showed that if a sufficiently large amount of planetesimal mass has been accumulated in a MMR, the planet feels perturbations from this material that cause new frequencies to appear in the planet's precession spectrum. These frequencies are near those of the resonant objects. Thus, the particles can resonate with frequencies in the planetary motion that they themselves induced, which produces large oscillations in their eccentricity. In this situation, Levison and Morbidelli (2003) showed that the resonant population can extend down to $e \sim 0$ even when the resonance has moved 10 AU past the edge of the disk.

Another complication to this story occurs if there are relatively large objects in the planetesimal disk that the planets are migrating through. Resonant capture requires that the migration of the planet is smooth. If the planet has jumps in semimajor axis due to the encounters with other planets or massive planetesimals, the locations of its MMRs jump as well. If the amplitude of these jumps is of order of the resonance width or larger, the particles trapped in the resonances will be released. A model of stochastic migration in planetesimal disks has been recently developed by Murray-Clay and Chiang (2005).

4. SIMPLE MIGRATION IN THE SOLAR SYSTEM

As described above, the magnitude and direction of planetesimal-driven migration is determined by a complex interaction of various dynamical sources and sinks of disk particles. Thus, this migration process is best studied through numerical experiments. In this section, we review what we know about the migration of the four giant planets of the solar system. Many researchers have studied this issue (Hahn and Malhotra, 1999; Gomes, 2003; GML04); however, we base our discussion on that in GML04.

4.1. Migration in Extended Disks

The simulations that follow all start with the following initial conditions. Jupiter, Saturn, Uranus, and Neptune are 5.45, 8.7, 15.5, and 17.8 AU, respectively. The planets are surrounded by a massive disk that extends from 18 AU to 50 AU and has a surface density variation as r^{-1} , which is the typically assumed value for protoplanetary disks (cf. Hayashi, 1981). The disk's outer edge was chosen to correspond to the current edge of the classical Kuiper belt (Allen et al., 2001a,b; Trujillo and Brown, 2001). The initial disk mass was varied between $40 M_{\oplus}$ and $200 M_{\oplus}$. The systems were evolved using the techniques in GML04 (see section 8).

Figure 2a shows a snapshot of the semimajor axis — eccentricity distribution of the planets and the planetesimals for the $50 M_{\oplus}$ simulation. Figure 2b shows the semimajor axes of the four giant planets with time. As discussed in section 2, Neptune, Uranus, and Saturn move outward, while Jupiter moves inward.

The black curves in Fig. 3 show the temporal evolution of Neptune's semimajor axis for runs of different disk masses. The $40 M_{\oplus}$ and $45 M_{\oplus}$ runs are example of damped migration (section 2). After a fast start, Neptune's outward motion slows down, and well before 10^9 yr, the planet reaches a quasi-asymptotic semimajor axis that is well within the outer edge of the disk. The part of the disk outside the orbit of Neptune preserves its original surface density, while the part interior to this distance is completely depleted.

A major change in Neptune's behavior occurs when the disk mass is increased $\geq 50 M_{\oplus}$. As before, Neptune experiences a fast initial migration, after which it slows down. Then it undergoes an approximately linear migration be-

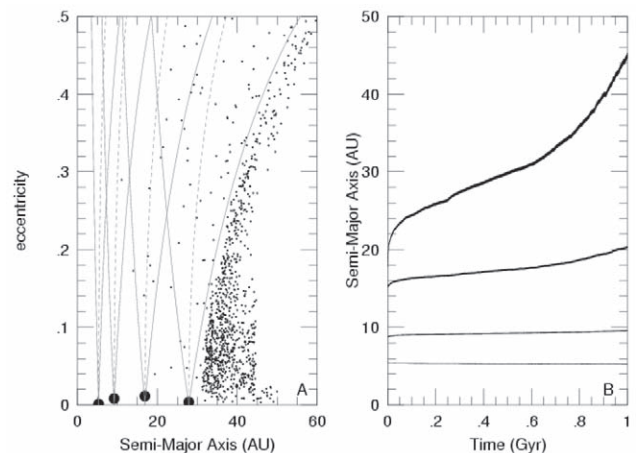


Fig. 2. Migration simulation from GML04 of the four giant planets in a $50 M_{\oplus}$ disk that extends to 50 AU. (a) A snapshot of the system at 330 m.y. Semimajor axis and eccentricity of the planets (filled dots) and of the planetesimals (points). The solid lines define the limits for planetary crossing orbits, while the dotted lines show where $H = H_p$ for zero-inclination orbits. (b) Evolution of the semimajor axes of the four giant planets.

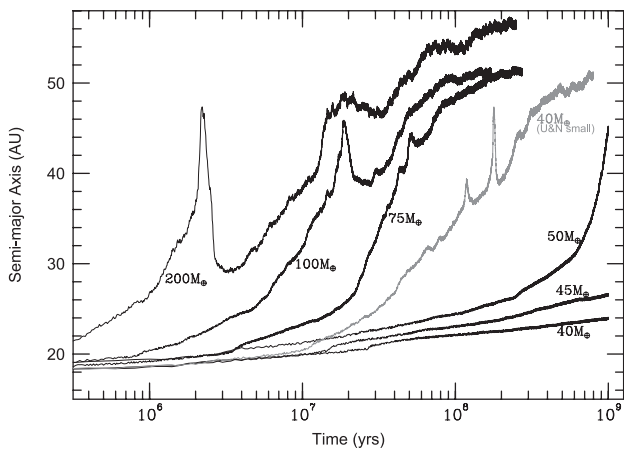


Fig. 3. The temporal evolution of Neptune’s semimajor axis for seven different simulations based on *GML04*. In all cases the disk was truncated at 50 AU, but the disk mass and the mass of the ice giants varied from run to run. In particular, the black curves show runs where the ice giants are their normal mass, while the one gray shows a run with Uranus and Neptune one-third of their current masses.

tween 100 and 600 m.y. Finally, Neptune’s migration accelerates toward the disk’s edge, where it eventually stops. This evolution suggests that the surface density of this disk is near a critical value that separates damped migration from sustained migration (see section 2). In all cases with more massive disks, Neptune final location was near the edge of the disk.

The transition from the linear to the accelerating phase in the 50- M_{\oplus} run is due to the variations in the number of particles trapped in Neptune’s MMRs. Recall from section 3 as Neptune migrates, disk particles become trapped in its MMRs. The resonant particles effect migration because they effectively increase Neptune’s inertial mass. During adiabatic migration, the number of particles in the resonances is roughly constant as long as the resonance is still in the disk. In this run, Neptune accelerates as its 1:2 MMR moves out of the disk probably because the number of objects in the resonance drops, new particles not being captured.

There is another important transition in Neptune’s behavior when the disk mass is increased to values larger than $\sim 100 M_{\oplus}$: The migration passes from a “forced” to a “runaway” mode. This change leads to a very interesting new phenomenon: Neptune’s migration is no longer monotonic. Figure 3 shows that in the case of the highest-mass disk, Neptune reaches ~ 50 AU in less than 3 m.y., and then comes back to within 30 AU almost equally as fast. Similar episodes of acceleration and return are also visible in other high-mass runs. This type of bounce is possible because, in runaway migration, objects are left behind in an excited disk as Neptune moves outward, instead of being transferred to the inner planets or ejected. When Neptune reaches the edge of the disk, the number of objects with $H > H_{\text{Nep}}$ drops, and so the remaining objects interior to Neptune can pull the

planet inward. Thus, Neptune reverses direction and starts a runaway *inward* migration. The same argument described above applies, so that this migration ends only when the region of the disk partially depleted by Uranus is encountered again. Notice however, that Neptune always ends up near the original edge of the disk at 50 AU.

Finally, the gray curve in the Fig. 3 shows a run in a 40- M_{\oplus} disk, but where the masses of the ice giants are one-third of their current values. Note that while migration is damped in a 40- M_{\oplus} disk when the ice giants are at their current mass, it is runaway in this case. This result shows that the transition between these two forms of migration occurs at a smaller disk mass for smaller planetary masses. This result gives an important constraint on the formation time of Uranus and Neptune. *Levison and Stewart (2001)* showed that standard planet-formation scenarios cannot form Uranus and Neptune in their current orbits, so these planets probably formed much closer to the Sun. However, if the ice giants would have migrated to their current orbits when they were much smaller then they are now, as the gray curve in the Fig. 3 suggests, how did they reach their current masses? This conundrum has a solution if the planets were fully formed when there was still enough gas in the system that the gravitational interactions with the gas prevented the planets from moving outward. This implies that these planets formed very early (≤ 10 m.y.) (*Podosek and Cassen, 1994; Hollenbach et al., 2000; Thi et al., 2001*), and is consistent with the capture of a primordial atmosphere of several Earth masses of H and He (*Pollack et al., 1996*).

4.2. Constraints from the Kuiper Belt

The question naturally arises whether we can determine what kind of migration actually occurred in the solar system, and from this the mass and structure of the original protoplanetary disk. In addition to the current orbits of the giant planets, the structure of the Kuiper belt supplies crucial clues to the solar system’s ancient history because this structure still carries the signatures of early evolution of the planetary system.

Three characteristics of the Kuiper belt are important: (1) The Kuiper belt only contains about $0.1 M_{\oplus}$ of material (*Jewitt et al., 1996; Chiang and Brown, 1999; Trujillo et al., 2001; Gladman et al., 2001; Bernstein et al., 2004*). This is surprising given that accretion models predict that $\geq 10 M_{\oplus}$ must have existed in this region in order for the objects that we see to grow (*Stern, 1996; Stern and Colwell, 1997a; Kenyon and Luu, 1998, 1999*). (2) The Kuiper belt is dynamically excited. Again, this is unexpected since accretion models predict that relative velocities between objects must have originally been small in order for the objects that we see to grow. (3) The Kuiper belt apparently ends near 50 AU (*Trujillo and Brown, 2001; Allen et al., 2001a,b*).

If we assume that the primordial Kuiper belt must have contained at least $\sim 10 M_{\oplus}$ between 40–50 AU in order to grow the observed objects, the above simulations suggest a scenario first proposed by *Hahn and Malhotra (1999)*. In

this model the disk contained $\sim 45 M_{\oplus}$ of material between 20 and 50 AU. Neptune started at ~ 22 AU and migrated to ~ 30 AU, where it stopped because its migration was damped. This left enough mass in the Kuiper belt to account for the growth of the known objects there. This scenario has a problem, however. If Neptune stopped at 30 AU because its migration was damped, how did the Kuiper belt lose $>99\%$ of its mass? Two general ideas have been proposed for the mass depletion of the Kuiper belt: (1) the dynamical excitation of the vast majority of Kuiper belt objects to the Neptune-crossing orbits after which they were removed, and (2) the collisional comminution of most of the mass of the Kuiper belt into dust.

GML04 studied Scenario (1), including the dynamical effects of the escaping Kuiper belt objects on Neptune. They concluded that any reasonable dynamical depletion mechanism would have forced Neptune to migrate into the Kuiper belt. Thus, Scenario (1) can be ruled out. Scenario (2) is also faced with some significant problems: (a) The orbital excitation of the cold classical Kuiper belt does not seem to be large enough to remove as much mass as is required (*Stern and Colwell, 1997b*); (b) substantial collisional grinding does not occur unless the physical strength of small Kuiper belt objects are extremely small (*Kenyon and Bromley, 2004*), much smaller than predicted by SPH collision calculations; and (c) most of the wide binaries in the cold population would not have survived the collisional grinding phase (*Petit and Mousis, 2004*). These problems led *GML04* to conclude that the collisional grinding scenario is also probably not viable.

4.3. Migration in Disks Truncated at 30 AU

GML04 argued that the current location of Neptune and the mass deficiency of the Kuiper belt imply that the protoplanetary disk possessed an edge at about 30 AU (see also *Levison and Morbidelli, 2003*). In their study of migration in such a disk, they found that a planet does not necessarily stop at the exact location of the edge. Indeed, since angular momentum must be conserved during the migration process, the final location of the planets depends more on the total angular momentum in the disk than on the location of the edge. To illustrate this, Fig. 4 shows Neptune’s migration in six disks that are initially spread between 10 and 30 AU, but with masses varying from 20 to $100 M_{\oplus}$.

The disk with $20 M_{\oplus}$ has a subcritical surface density. Neptune exhibits a damped migration and stalls well within the disk. Therefore a massive annulus is preserved between a few AU beyond the planet’s location and the original outer edge of the disk. The disks with $30 M_{\oplus}$ and $35 M_{\oplus}$ have a surface density close to the critical value. In both cases, when the planet reaches ~ 26 AU, the unstable region of the disk [which extends up to a distance of about one-sixth of the planet’s semimajor axis (*Duncan et al., 1995*)] reaches the edge of the disk. The planet starts to feel the disk truncation and its migration is rapidly damped. The final location is 2 AU inside the original disk edge, but the entire

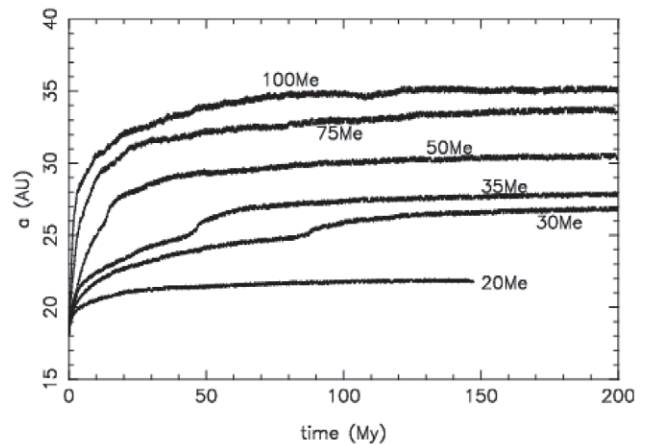


Fig. 4. Examples of Neptune’s migration in disks with an outer edge at 30 AU and masses equal to between 20 and $100 M_{\oplus}$. Reproduced from *GML04* (their Fig. 10). Note that a direct comparison cannot be made between these total masses and those in the runs shown in Figs. 2 and 3 because the disk was larger in the earlier runs.

region beyond the planet has been depleted. More massive disks have supercritical densities. In the case of $50 M_{\oplus}$ the planet stops almost exactly at the disk’s edge, while in the other cases it goes several AU beyond it.

Thus, *GML04* concluded that a disk with an outer edge close to 30 AU, the exact value depending on the disk’s mass, can explain Neptune’s current semimajor axis. There are at least five mechanisms that could have truncated the disk at such a small heliocentric distance, prior to planetary accretion: (1) A passing star tidally strips the Kuiper belt after the observed Kuiper belt objects formed (*Ida et al., 2000; Kobayashi and Ida, 2001; Levison et al., 2004*). (2) An edge formed prior to planetesimal formation due to aerodynamic drag (*Youdin and Shu, 2002*). (3) An edge formed during planet accretion due to size-dependent radial migration caused by gas drag (*Weidenschilling, 2003*). (4) Nearby early-type stars photoevaporated the outer regions of the solar nebula before planetesimals could form (*Hollenbach and Adams, 2004*). (5) Magnetohydrodynamic instabilities in the outer regions of the disk prevented the formation of planetesimals in these regions (*Stone et al., 1998*). We stress that a small truncation radius is *not* in contradiction with the existence of the Kuiper belt beyond 40 AU. In fact, the entire Kuiper belt could have been pushed out from within the disk’s edge during Neptune’s migration. We return to the issue of the Kuiper belt in section 6.

5. DYNAMICAL INSTABILITIES AS A MIGRATION PROCESS

Up to this point we have been discussing “simple” migration. However, there is another way in which the interaction between planets and small bodies can result in a large change in the planetary radial distribution. First, a global

instability in the planetary system increases the planets' eccentricities and semimajor axis separations; then, the interaction between the disk particles and the planets circularize the planetary orbits. Eventually, a final phase of "simple" migration can follow.

The above idea was first suggested by *Thommes et al.* (1999). They postulated that the four giant planets formed in such a compact configuration that their orbits were dynamically unstable. Plate 5 shows four snapshots from one of *Thommes et al.*'s (1999) simulations, where the ice giants were hypothesized to have formed between Jupiter and Saturn. Almost immediately ($\sim 10^4$ yr), the ice giants are scattered out from between Jupiter and Saturn into a pre-existing planetesimal disk, where gravitational interactions with the disk particles eventually circularize their orbits. The gravitational interaction between the planetesimals and the scattered cores comes in two flavors. First, there is a secular response by the disk to the eccentricities of the ice giants. This can clearly be seen in the lower left panel of the figure ($t = 180,000$ yr), where the objects between 20 and 30 AU have their eccentricities systematically pumped. Since this region of the disk is more massive than the ice giants, this secular response lifts the perihelion distances of the ice giants away from Saturn's orbit, thus saving them from ejection into interstellar space. Second, *dynamical friction*, which occurs as a large object is moving through a sea of background particles (*Chandrasekhar*, 1943; although see *Binney and Tremaine*, 1987, for a discussion), further circularizes the ice giants' orbits. The problem with the evolution illustrated in Plate 5 is that disks massive enough to circularize the ice giants typically force them to migrate too far. We address this issue in the next section.

6. THE NICE MODEL OF THE EARLY DYNAMICAL EVOLUTION OF THE GIANT PLANETS

A new model of the dynamical evolution of the outer solar system has been presented in a recent series of papers (*Tsiganis et al.*, 2005, hereafter *TGML05*; *Morbidelli et al.*, 2005a, hereafter *MLTG05*; *Gomes et al.*, 2005, hereafter *GLMT05*). This is the most comprehensive model to date and it reproduces most of the characteristics of the outer planetary system at an unprecedented level. We refer to this model as the "Nice model" because it was developed at the Nice Observatory. Since it makes use of many of the ideas explored in this chapter, we describe it in detail below.

6.1. The Dynamical Evolution of Giant Planet Orbits

The initial motivation for the Nice model was the desire to understand the orbital eccentricities and inclinations of Jupiter and Saturn, which can reach values of $\sim 10\%$ and $\sim 2^\circ$, respectively. Planetary formation theories suggest that these planets should have formed on circular and coplanar orbits. In addition, the final stage of planetesimal-driven

migration, which is the topic of this chapter, quickly damps any preexisting eccentricities and inclinations. Thus, the initial work that led to the Nice model was a set of simulations intended to solve the mystery of the origins of Jupiter and Saturn's eccentricities and inclinations.

In particular, the hypothesis studied in *TGML05* was that orbital excitation could take place if, during migration, two planets crossed a low-order MMR. Saturn is currently located interior to the 2:5 MMR and exterior to the 1:2 MMR with Jupiter. If the initial planetary configuration was initially sufficiently compact, then — given that these two planets had to migrate on opposite directions — they would have crossed their 1:2 MMR, which is the strongest of the MMRs.

TGML05 performed a series of numerical integrations of the above idea. In all these simulations the four giant planets were started on nearly circular and coplanar orbits, with Saturn placed a few tenths of an AU interior to the 1:2 MMR. Starting Saturn interior to the resonance is a basic assumption of the Nice model. However, recent hydrodynamical simulations of two planets embedded in a gaseous disk (*Morbidelli et al.*, 2005b) not only suggest that this assumption is reasonable, but may even be required if one wants to avoid migrating Jupiter into the Sun via planet-gas disk interactions. However, whether reasonable or not, the Nice model can only valid if this assumption is true. *TGML05* initially placed the ice giants just outside Saturn's orbit. The planets were surrounded by massive disks containing between 30 and 50 M_\oplus of planetesimals, truncated at ~ 30 AU.

The typical evolution from *TGML05* is shown in Fig. 5. After a phase of slow migration, Jupiter and Saturn encounter the 1:2 MMR, at which point their eccentricities jumped to values comparable to the ones currently observed, as pre-

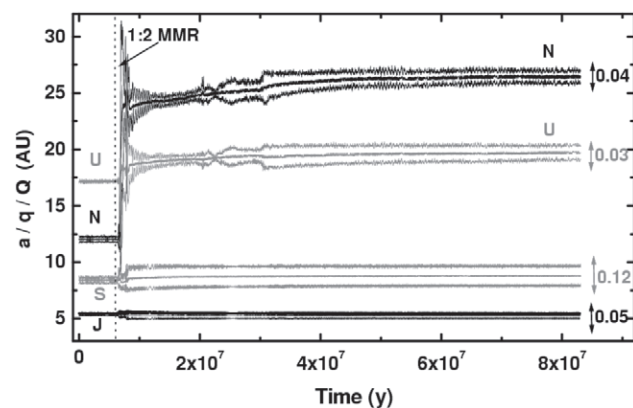


Fig. 5. Orbital evolution of the giant planets from one of *TGML05*'s N-body simulations. The values of a , q , and Q are plotted for each planet. The separation between the upper and lower curves is a measure of the eccentricity of the orbit. The maximum eccentricity of each orbit, computed over the last 2 m.y. of evolution, is noted on the plot. The vertical dotted line marks the epoch of 1:2 MMR crossing. The planetesimal disk contained initially 35 M_\oplus . Reproduced from *TGML05* (their Fig. 1).

dicted by adiabatic theory. The sudden jump in the eccentricities of Jupiter and Saturn has a drastic effect on the planetary system as a whole. The perturbations that Jupiter and Saturn exert on Uranus and Neptune force the ice giants' orbits to become unstable. Both ice giants are scattered outward and penetrate the disk (although less violently than in the simulation presented in section 5). Then the eccentricities and inclinations of the ice giants are damped by the disk as described in section 5, and the planetary system is stabilized. The planets stop migrating when the disk is almost completely depleted. As shown in Fig. 5, not only their final semimajor axes, but also their final eccentricities are close to the observed values. In this run, the two ice giants exchange orbits. This occurred in $\sim 50\%$ of *TGML05*'s simulations.

TGML05 found that in roughly 70% of their simulations both ice giants were saved from ejection by the planetesimal disk and evolved onto nearly-circular orbits. They divided these so-called “successful” runs into two groups: (1) those in which there were no encounters between an ice giant and a gas giant, and (2) those in which Saturn suffered encounters with one or both ice giants. Figure 6 shows the mean and standard deviation of the orbital elements for group (1), in gray, and group (2), in black. The orbital elements for the real planets are also shown as filled black dots. When no encounters with Saturn occur, the final eccentricities and inclinations of the planets, as well as the semimajor axis of Uranus, tend to be systematically smaller than the observed values. On the other hand, when distant encounters between Saturn and one of the ice giants also occurs, the final planetary system looks very similar to the actual outer solar system. This is the first time that a numerical model has quantitatively reproduced the orbits of the giant planets of the solar system.

Although there are many free parameters in the initial conditions of the Nice model (for example, the initial orbits of the planets, the mass of the disk, and the inner and outer edges of the disk), there are only two that effect the final location of the planets. The first is the assumption that the disk was truncated near 30 AU. As described above, *TGML05* made this assumption in order to circumvent the Kuiper belt mass-depletion problem. The only other parameter important in determining the orbits of the planets is the initial mass of the disk. All other parameters mainly affect the timing of the resonance crossing, a fact used in section 6.3, but not the final orbits of the planets themselves.

TGML05 also found a systematic relationship between final orbital separation of Jupiter and Saturn at the end of migration and the initial mass of the disk. For disk masses larger than $\sim 35\text{--}40 M_{\oplus}$, the final orbital separation of Jupiter and Saturn tends to be larger than is actually observed. Indeed, for disks of $50 M_{\oplus}$, Saturn was found to cross the 2:5 MMR with Jupiter. In addition, the final eccentricities of the two gas giants were too small, because they had experienced too much dynamical friction. Thus, an initial disk mass of $\sim 35 M_{\oplus}$ was favored. The fact both the semimajor axes and the eccentricities/inclinations of Jupiter and

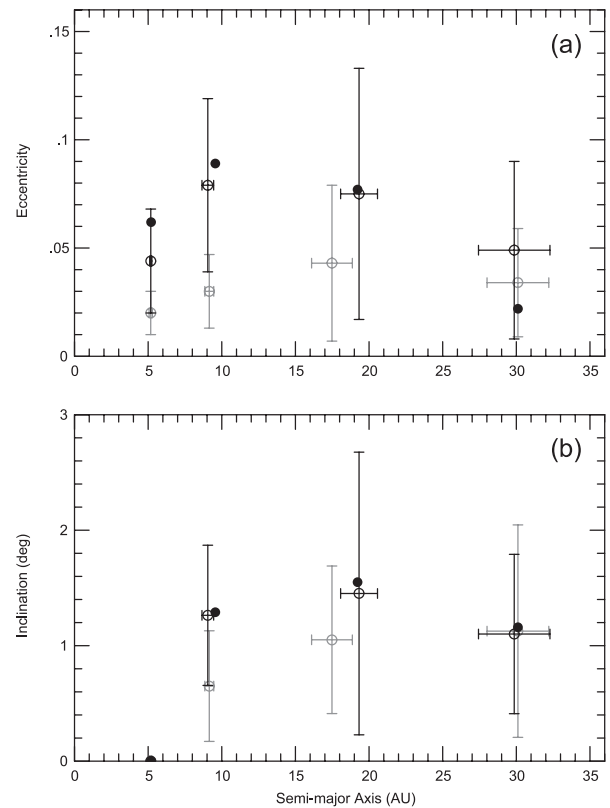


Fig. 6. Comparison of *TGML05*'s synthetic final planetary systems with the outer solar system. **(a)** Proper eccentricity vs. semimajor axis. **(b)** Proper inclination vs. semimajor axis. Proper eccentricities and inclinations are defined as the maximum values acquired over a 2-m.y. timespan and were computed from numerical integrations. The inclinations are measured relative to Jupiter's orbital plane. These values for the real planets are presented with filled black dots. The open gray dots mark the mean of the proper values for the runs of group 1 (no encounters for Saturn), while the open black dots mark the same quantities for the runs of group 2. The error bars represent 1σ of the measurements. Reproduced from *TGML05* (their Fig. 2).

Saturn are reproduced in the same integrations strongly supports this model: There is no *a priori* reason that a , e , and i should all be matched in the same runs.

6.2. Small-Body Reservoirs

Further support for the Nice model comes from the small-body reservoirs. Indeed, jovian Trojans, which are small objects in the 1:1 MMR with Jupiter, supply an important test for *TGML05*'s scenario. *Gomes (1998)* and *Mich-tchenko et al. (2001)* studied the effects of planetesimal-driven migration on the Trojan asteroids. They found that the Trojans were violently unstable if Jupiter and Saturn crossed the 1:2 MMR with one another. Thus, these authors concluded the Jupiter and Saturn could *not* have crossed this resonance. So, is *TGML05* wrong?

The issue was addressed in the second of the three Nice model papers, *MLTG05*. The authors of this paper pointed out that the dynamical evolution of any gravitating system is time reversible. So, if the planetary system evolves into a configuration so that trapped objects can leave the Trojan points, it must be possible that other bodies can enter the same region and be temporally trapped. Consequently, a transient Trojan population can be created if there is a source for these objects. In this case, the source is the very bodies that are forcing the planets to migrate. When Jupiter and Saturn get far enough from the 2:1 MMR so that the coorbital region becomes stable again, the population that happens to be there at that time remains trapped, becoming the population of permanent jovian Trojans.

MLTG05 performed a series of N-body simulations to study this idea and found that bodies can indeed be permanently captured in Trojan orbits. Assuming that the original planetesimal disk contained $35 M_{\oplus}$ (as in *TGML05*), they predict that there should be between $\sim 4 \times 10^{-6} M_{\oplus}$ and $\sim 3 \times 10^{-5} M_{\oplus}$ of Trojans with libration amplitude $D < 30^\circ$. This can be favorably compared to the total mass of the Trojans, which, using data from the Sloan Digital Sky Survey and updated numbers on density and albedo, was reevaluated by *MLTG05* to be 1.1×10^{-5} (also see discussions by *Jewitt et al., 2000; Yoshida and Nakamura, 2005*). One of the surprising aspects of the Trojan population is its broad inclination distribution, which extends up to $\sim 40^\circ$ and cannot be explained by traditional capture scenarios. *MLTG05* finds that they can reproduce this as well. Since this model is the only one available that can explain these features, the Trojans represent observational evidence for the 1:2 resonance crossing proposed by *TGML05*.

Jupiter is not the only planet in the outer solar system that has Trojan asteroids. Neptune currently is known to have four such objects. These objects are also explained by the Nice model. *TGML05* found that objects can be trapped in Neptune's 1:1 MMR during the time when Neptune's eccentricity is being damped by the planetesimal disk. Indeed, the Nice model supplies the only known Neptune Trojan formation mechanism that can explain the high inclination (25°) of 2005 TN₅₃. [For example, the most widely quoted model, *Chiang and Lithwick (2005)*, does not accomplish this.]

The Kuiper belt also presents an important test of the Nice model. Any model of the outer solar system evolution must explain the main orbital properties of the Kuiper belt objects (see *Morbidelli et al., 2003*, for a review): (1) the presence of objects trapped in Neptune's MMRs (some shown as gray vertical lines in Fig. 7a); (2) the abrupt end of the *classical* Kuiper belt at or near the location of the 1:2 MMR [we define as the classical Kuiper belt the collection of objects that are nonresonant and fall below the stability limit determined by *Duncan et al. (1995)*, shown by a gray curve in Fig. 7a]; (3) the dearth of objects with $45 \leq a \leq 48$ AU and $e < 0.1$; (4) the apparent coexistence in the classical Kuiper belt of two populations: a dynamically *cold* population — made of objects on orbits with inclinations $i < 4^\circ$ — and a *hot* population — whose incli-

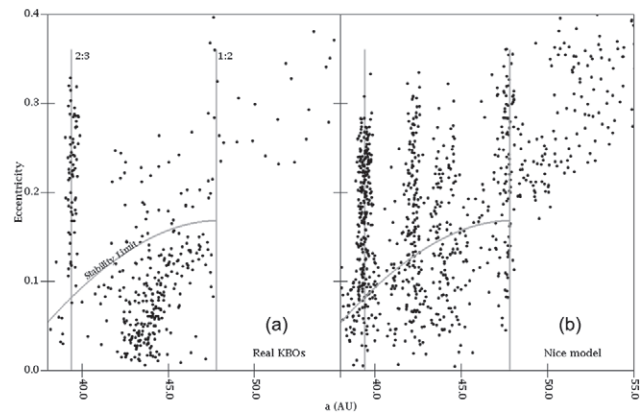


Fig. 7. The eccentricity-semimajor axis distribution of objects in the Kuiper belt. The dots show the objects. The two vertical gray lines show Neptune's 2:3 MMR and 1:2 MMR. The gray curve shows a stability limit determined by *Duncan et al. (1995)*. **(a)** The real multi-opposition Kuiper belt objects, as released by the MPC in November 2005. **(b)** Resulting distribution 1 G.y. after the 1:2 MMR planetary instability, from our new dynamical model based on the Nice scenario.

nations can be as large as 30° , and possibly larger (*Brown, 2001*). These populations have different size distribution (*Levison and Stern, 2001; Bernstein et al., 2004*) and different colors (*Tegler and Romanishin, 2003; Trujillo and Brown, 2002*).

The investigation of the formation of the Kuiper belt in the framework of the Nice model is in progress, and we briefly discuss here the preliminary, unpublished results.

For reasons discussed above, the Nice model assumes that the protoplanetary disk was truncated near ~ 30 AU. This implies that the Kuiper belt that we see today had to be pushed outward from the initial disk during Neptune's orbital evolution. The envisioned mechanism is the following. When Neptune becomes eccentric ($e_N \sim 0.3$) many of its MMRs are very wide. Numerical simulations show that for $e_N > 0.2$, the entire region inside the 1:2 MMR is covered with overlapping resonances and thus is entirely chaotic. Consequently, it fills with disk particles scattered by Neptune. As Neptune's eccentricity damps, many of these particles become permanently trapped in the Kuiper belt. Resonances do not overlap beyond the 1:2 MMR and thus this resonance forms a natural outer boundary for the trapped population.

Figure 7b shows the result of this process according to a set of new numerical simulations we performed to study the above idea. First, note that most of the nonresonant particles above the stability curve would be lost if the simulation were carried until 4 G.y. Given this, there is remarkably good agreement between the two populations. There is an edge to the main Kuiper belt at the location of the 1:2 MMR. In addition, the resonance populations are clearly seen. The latter are not acquired by the resonances via the standard migration capture scenario of *Malhotra (1993, 1995)*, but by the mechanism proposed by *Gomes (2003)*.

The model in Fig. 7b also reproduces the dearth of low-eccentricity objects beyond ~ 45 AU. The inclination distribution of the main Kuiper belt is also a reasonable match to the data. This model predicts that roughly 0.1% of the original disk material should currently be in the Kuiper belt. Assuming an initial disk mass of $35 M_{\oplus}$ (as in *TGML05*) leads to a Kuiper belt mass of $0.04 M_{\oplus}$, which is consistent with observations. And finally, there is a crude correlation between the formation location in the planetesimal disk and the final Kuiper belt inclination for a particle. This relationship might be able to explain the observed relationship between physical characteristics and Kuiper belt inclination. This work is not yet complete. However, it seems to explain many of the characteristics of the Kuiper belt with unprecedented quality, thus also supporting the framework of the Nice model.

6.3. The Lunar Late Heavy Bombardment

The “late heavy bombardment” (LHB) was a phase in the impact history of the Moon that occurred roughly 3.9 G.y. ago, during which the lunar basins with known dates formed. There is an ongoing debate about whether the LHB was either the tail-end of planetary accretion or a spike in the impact rate lasting ≤ 100 m.y. [“terminal cataclysm” (*Tera et al.*, 1974)]. Although the debate continues, we believe that there is growing evidence that the LHB was indeed a spike. The LHB was recently reviewed in *Hartmann et al.* (2000) and *Levison et al.* (2001).

A spike in the impact flux in the inner solar system most likely required a major upheaval in the orbits of the planets that destabilized one or more small-body reservoirs, which, until that time, had been stable (cf. *Levison et al.*, 2001). The Nice model naturally provides such an upheaval when Jupiter and Saturn cross the 1:2 MMR. The problem investigated in *GLMT05* (the third paper in the Nice trilogy) was how to delay the resonance crossing for ~ 700 m.y. In the simulations in *TGML05*, planet migration started immediately because planetesimals were placed close enough to the planets to be violently unstable. While this type of initial condition was reasonable for the goals of that work, it is unlikely. Planetesimal-driven migration is probably not important for planetary dynamics as long as the gaseous massive solar nebula exists. The initial conditions for the migration simulations should represent the system that existed at the time the nebula dissipated, i.e., one in which the dynamical lifetime of the disk particles is longer than the lifetime of the nebula. *GLMT05* found that for planetary systems like those used as initial conditions in the Nice model, this inner edge of the planetesimal disk is roughly 1 AU beyond the orbit of the outermost ice giant.

In this configuration, *GLMT05* found that the 1:2 MMR crossing was delayed by between 350 m.y. and 1.1 G.y., depending on various parameters. They concluded that the global instability caused by the 1:2 MMR crossing of Jupiter and Saturn could be responsible for the LHB, since the estimated date of the LHB falls in the range of the crossing times that they found. *GLMT05* also found that, for an

initial disk mass of $35 M_{\oplus}$ (as in *TGML05*), after the resonance crossing roughly 8×10^{21} g of cometary material impacted the Moon. This value is consistent with the estimate of $\sim 6 \times 10^{21}$ g from the observed basins (*Levison et al.*, 2001). Moreover, the asteroid belt would have been perturbed during this event, thereby supplying additional impactors. Overall, this material arrived over a relatively short period of time (~ 50 m.y.). Thus, this model produces a spike in the impact rate of about the correct duration.

One of the requirements of *GLMT05*'s model is that the mass of external planetesimal disk not significantly evolve between the time when the solar nebula disperses and the time of the LHB. In principle, the disk mass can change as a result of either the action of dynamics or the action of collisions, although the simulations in *GLMT05* already show that dynamics are not a factor. A preliminary study of the collisional evolution of such a disk by *O'Brien et al.* (2005) suggests that there is a reasonable range of parameters over which the primordial transneptunian disk is able to remain massive ($\sim 35 M_{\oplus}$) for 700 m.y. In addition, the final size distribution of transneptunian bodies in these calculations is consistent with that inferred for the Kuiper belt by *Bernstein et al.* (2004). However, it should be noted that *O'Brien et al.* (2005) studied only a small fraction of the available parameter space and thus more such studies are necessary in order to settle this issue.

At this juncture, let us take stock of the Nice model. It quantitatively reproduces the semimajor axes, eccentricities, and inclinations of the giant planets. In addition, it reproduces the Trojan asteroids of both Jupiter and Neptune. Indeed, it reproduces, for the first time, the orbits of Jupiter's Trojans and quantitatively predicts the amount of material that should be in this population. It also is the most successful model to date at reproducing the total mass and orbital distribution of the Kuiper belt. It accomplishes all this with very few important free parameters. As described in section 6.1, if one accepts the need to truncate the initial planetesimal disk at 30 AU, the initial disk mass is the only parameter that significantly affects these results. It is a strength of the Nice model that a single value of disk mass ($35 M_{\oplus}$) can produce all the characteristics we just listed. And finally, as *GLMT05* has shown, this model quantitatively reproduces the so-called late heavy bombardment of the Moon. These accomplishments are unparalleled by any other model. Not only is there no other model that can explain all these characteristics, but the level of agreement between the model and observations is unprecedented.

7. MIGRATION IN EXTRASOLAR PLANETESIMAL DISKS

In this section we discuss some behaviors that planets might have followed in extrasolar planetesimal disks. It is very difficult, if not impossible, to be exhaustive because, as we saw in section 2, planet migration in planetesimal disks depends crucially on the specific features of the system: the number of planets, their separations, their masses and mass ratios, the disk's mass and radial extent, its radial

surface density profile, etc. Thus, we concentrate only on four main aspects: the origin of warm Jupiters, the evolution of two-planet systems, the runaway of medium-mass planets out to very large distances from the parent star, and the triggering of late instabilities.

7.1. Planetesimal-driven Migration and the Origin of Hot and Warm Jupiters

We have seen in section 2 that a single giant planet (of about $1 M_{\text{Jup}}$ or more) embedded in a planetesimal disk migrates inward, because it ejects most of the planetesimals that it interacts with. Assuming a minimal mass planetesimal disk [the solid component of the *Hayashi* (1981) minimum mass nebula], *Murray et al.* (1998) found that Jupiter would have had a very damped migration, so that it would not have moved significantly. However, if the density of the disk is enhanced by a large factor (15–200), *Murray et al.* showed that the migration can be in a runaway mode. This can push the planet inward to distances from the central star that are comparable to those observed in extrasolar systems.

Although extremely massive disks are required to produce the so-called “hot Jupiters” ($a \leq 0.1$ AU), more moderate (but still massive) disks can produce the “warm Jupiters” ($a \sim 1$ AU). In particular, the advantage of planetesimal-driven migration over gas-driven migration for the origin of warm Jupiters is that the stopping mechanism is much more natural. If the radial surface density profile of the planetesimal disk is shallower than $1/r^2$, the runaway migration turns eventually into a damped migration, as the planet moves inward. Thus, the planet suddenly stops.

7.2. Migration in Two-Planet Systems

Two-planet systems are interesting because they have many of the characteristics of systems with a larger number of planets. Thus, insight into the behavior of systems, in general, can be gained by studying systems with two planets. Unfortunately, as explained above, it is not possible to completely explore this issue because of the large number of parameters involved. In this subsection, we investigate with new, unpublished simulations the case of two giant planets in the current orbits of Jupiter and Saturn with a disk stretching from 6 to 20 AU containing a total mass of $1.2\times$ that of the sum of the masses of the planets. Thus, in all cases the system is in the *forced* migration mode. When Jupiter and Saturn have their current masses, Jupiter migrates inward and Saturn outward (the black curves in Plate 6a), just like in the four-planet case.

In the first series of runs, we looked at the effect that the total mass of the planets has on migration. It might be expected that in a system with two massive planets, the outer one ejects more particles than it passes to the inner one and thus both planets migrate inward. However, our simulations show that the above expectation is not correct. By scaling the mass of the disk and of the planets by factors of 3 and 10, we obtain the evolutions shown by the blue

and red curves in Plate 6a, respectively. These behaviors are similar to one another, the migration timescale being the only significant difference. We believe that the above argument is wrong because, although encounters are more common for larger planets due to their larger gravitational cross-sections, the relative distribution of velocity changes is roughly independent of mass. The larger gravitational cross-sections for the more massive planets lead to the faster migration times, not to a different evolutionary pattern.

In the second series of runs, we kept the total mass of the planets constant ($3\times$ the summed masses of Jupiter and Saturn), but varied their mass ratio. The results of these simulations are shown in Plate 6b for systems where the ratio of the mass of the inner planet to that of the outer ranged from 0.5 to 3.3. We find that for mass ratios ≥ 2 , the outer planet always migrates outward. However, for mass ratios less than roughly 2, the inner planet becomes less effective at removing particles crossing the orbit of the outer planet, and thus the outer planet is more likely to eject them. Thus, after a short period of outward migration, the outward planet migrates inward. Also note that, for at least the conditions studied here, the outer planet inward migration is faster than that of the inner planet. These results suggest that planetesimal migration can lead to resonant trapping between giant planets, as is observed in many extrasolar planetary systems (*Schneider*, 2004). It could also drive a planetary system into an unstable configuration.

7.3. Driving Planets Far from Their Star

Most of the observed debris disks show features like gaps, warps, asymmetric clumps, and even spiral waves, usually attributed to the presence of embedded planets. For instance, *Wyatt* (2003) showed that the features of the Vega disk could be due to a Neptune-mass planet migrating from 40 to 65 AU in 56 m.y. Similarly, *Wyatt et al.* (2005) modeled the observations of the η Corvi disk with a Neptune-mass planet moving from 80 to 105 AU in 25 m.y. Other features in the β Pictoris (*Wahhaj et al.*, 2003) and ϵ Eridani disks (*Ozernoy et al.*, 2000; *Greaves et al.*, 2005) have been modeled with planets at several tens of AU. In the most extreme model, the spiral features of the HD141569 disk have been modeled with one planet of $0.2\text{--}2 M_{\text{Jup}}$ at ~ 250 AU and a Saturn-mass planet at 150 AU (*Wyatt*, 2005). These models call for an exploration of the possibility that planets migrate very far from the central star.

We have seen in section 4 that if our planetary system had been embedded in a massive disk truncated at 50 AU, Neptune would have had migrated very quickly in the runaway mode to the edge of the disk. Figure 8 shows the evolution of Neptune if the same disk were extended to 200 AU, with a radial surface density profile $\propto 1/r$. Neptune reaches a heliocentric distance larger than 110 AU. Then, without having reached the edge of the disk, it bounces back, reversing its migration direction. This abrupt change in the migration behavior happens because, when the planet migrates sufficiently fast, the timescale for planetesimals encountering the planet becomes comparable to, or longer

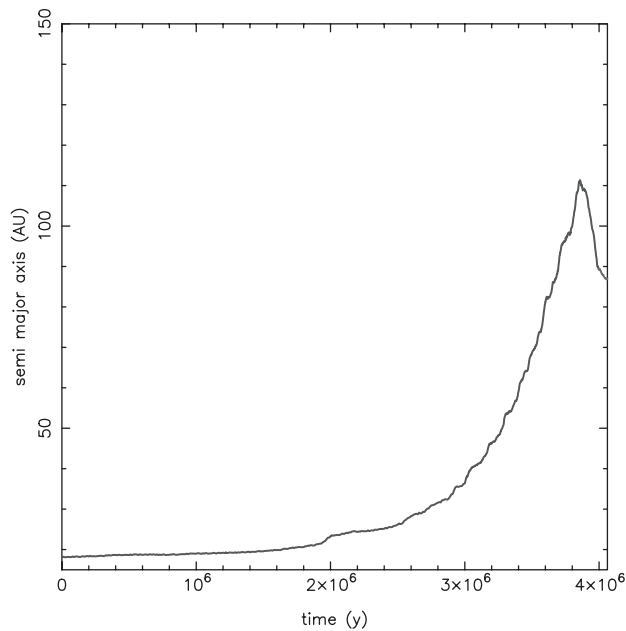


Fig. 8. The migration of Neptune in a very massive planetesimal disk, extended from 20 to 200 AU and with $6 M_{\oplus}$ of material in each AU-wide annulus. From *GML04*.

than, that for passing through the planet-crossing region due to the migration of the planet itself. So, in coordinates that move with the planet, most particles simply drift inward while keeping their eccentricities roughly constant. The net result is that \bar{k} in equation (2) gradually decreases with time.

The planet does not respond to the reduction of \bar{k} by gradually slowing down its migration because, contemporaneously, the amount of mass in the planet-crossing region (M in equation (2)) increases at a faster rate than \bar{k} decreases. Consequently, the magnitude of \dot{a}_p does not decrease with time. However, when $\bar{k} = 0$, \dot{a}_p becomes zero and the migration abruptly stops. When this happens, the planet finds itself in an unstable situation. If the excited disk interior to planet slightly overpowers the particles from the outer disk, the planet initiates a runaway migration inward.

It is worth stressing, however, that the kind of migration illustrated in Fig. 8 most likely only works for medium-mass planets, like Neptune. Moving a planet as large as Jupiter with a planetesimal disk probably requires a disk that is too massive to be believable.

7.4. Late Instabilities

The striking success of the Nice model for the early evolution of the solar system (see section 6) suggests that gravitational instabilities can be very important in the history of a planetary system. Another piece of evidence comes from outside the solar system. Many of the known extrasolar planets are on very eccentric orbits. It has been argued the most natural explanation for this astonishing result is that these systems also suffered from a violent, global rearrangement of their planets' orbits (*Rasio and Ford, 1996*;

Weidenschilling and Marzari, 1996; *Levison et al., 1998*; *Papaloizou and Terquem, 2001*; *Moorhead and Adams, 2005*).

Why do planetary systems become unstable? There is nothing in the physics of the planet-formation process that guarantees that a planetary system will be stable on a time-scale longer than that characterizing planet formation itself. Thus, a planetary system could remain quiescent for hundreds of millions of years and then become completely unstable (*Levison et al., 1998*).

As the Nice model and the runs in section 7.2. illustrate, it is also possible that the gravitational interaction between the planets and a massive small-body reservoir could drive a planetary system into an unstable configuration. In fact, it could be quite generic that, at the end of the gas-disk phase, planetesimals are only on orbits with a dynamical lifetime longer than the nebula dissipation time, hence driving a *slow* migration that leads, at some point, to instability. Thus, late heavy bombardments may not be the rule, but we can expect them to occur in a fairly good fraction of the multiplanet systems.

Indeed, the recent Spitzer observation of the SEDs of nearby main-sequence A stars (*Rieke et al., 2005*) and solar-type stars (*Kim et al., 2005*) revealed some main-sequence systems with ages between 100 m.y. and 3 G.y. that have unexpectedly bright infrared excesses indicating large amounts of circumstellar dust. The A-star sample included systems with ages in the few $\times 100$ m.y. range that have 24- μ m flux densities 1.5–2 \times brighter than predicted for the stellar photospheres alone. Those excesses correspond to bolometric fractional luminosities $L_{\text{dust}}/L_{\text{star}}$ of a few $\times 10^{-4}$ for estimated dust temperatures of 75 to 175 K, i.e., the dust intercepts that fraction of the central star's total output and reradiates the energy into the thermal IR. For A stars those dust temperatures correspond roughly to radii of 10 to 60 AU. The minimum mass of dust required to produce those excesses is on the order of only 10^{20} kg, equivalent to a single object a few hundred kilometers in diameter.

Similarly, the solar-type star sample showed that more than 15% of systems with ages into the gigayear range have IR excesses prominent at 70 μ m, corresponding to temperatures of roughly 40 to 75 K and “Kuiper belt-like” radii of 20 to 50 AU. Note that the minimum dust masses required to produce prominent excesses at lower temperatures and longer wavelengths around the solar-type stars are typically 10^{-3} – $10^{-2} M_{\oplus}$, 2 orders of magnitude larger than for the A stars. A total planetesimal mass of 3–10 M_{\oplus} is required to produce that much dust in collisional equilibrium for a belt with dimensions like our Kuiper belt. That mass range is deduced by either scaling limits on Kuiper belt mass from IR flux limits for a regime in which P-R drag dominates dust dynamics (*Backman et al., 1995*), or by scaling dust mass to parent-body mass for a collision-dominated regime.

An inferred belt mass of 3–10 M_{\oplus} is significant because evolution solely by collisional grinding of a Kuiper belt-sized system cannot produce both the amount of dust that we see and as massive a remnant after 1 G.y.: To produce this much dust, the planetesimals have a collisional evolu-

tion timescale an order of magnitude shorter than the system age. Thus, the exceptional systems observed in these samples are certainly not the late stages of ordinary evolution of originally supermassive planetesimal belts. Instead they must represent either recent single large collisions of lunar-mass bodies, or possibly more common late-epoch instabilities like our solar system's LHB (see also chapter by Meyer et al.).

8. CAVEATS AND LIMITATIONS OF NUMERICAL SIMULATIONS

Much of the information presented in this chapter is based on examples taken from numerical simulations. Thus, a natural question arises about the reliability of such calculations. Modern simulations of planet migration are performed using symplectic N-body integrators (*Duncan et al., 1998; Chambers, 1999*), which have very good conservation properties for energy and angular momentum, even during close encounters. However, even with modern computers some simplifications are required in order to make these calculations feasible. In particular, the disk is usually modeled with only 1000–10,000 equal mass particles, which interact gravitationally with the planets but do not interact with each other. This method of handling the disk has three main limitations.

First, the typical mass of an individual disk particle in the simulation is on the order of 0.005–0.1 M_{\oplus} , depending on the total mass of the disk and the number of particles used. Even if we cannot exclude the presence of bodies with the mass of the Moon (0.01 M_{\oplus}) or even of Mars (0.1 M_{\oplus}) in the disk, they probably carry only a small fraction of the total disk mass. Thus, the individual particle mass used in these simulations is definitely unrealistic. As we have seen in section 3, large disk particles lead to a stochastic component of planet migration, and thus if the disk particles are unreasonably large, there could be a spurious component to the migration. This stochasticity affects the capture of particles in resonances and their subsequent release. In turn, this has an impact not only on the disk's structure, but also on the mean planet migration rate. In addition, the stochastic oscillation of the planet's semimajor axis tends to sustain the migration even in cases where, in reality, the migration should be damped. *GML04* showed examples where Neptune's migration is damped in 40- M_{\oplus} or 45- M_{\oplus} disks modeled with 10,000 particles (see Fig. 3), but is in a forced mode when the same disks are modeled using only 1000 particles. *GML04* argued, however, that a disk of a few thousand particles is most likely adequate for most simulations.

In any case, whenever an interesting dynamical phenomenon is observed in the disk, it is good practice to check if the phenomenon persists in a simulation where the disk's particles are massless, and the planets are forced to migrate by including a suitable drag term in the planet's equations of motion (e.g., *Malhotra, 1993*). If the phenomenon persists, then it is most likely real. However, if it disappears,

then it should be viewed with some skepticism and further tests should be done.

A second limitation with our techniques is the lack of gravitational interactions among the disk particles. We see two possible implications of this simplification. First, the precession rates of the orbits of the particles are incorrect, and thus the locations of secular resonances are wrong. It is very difficult to prevent this error, unless the mutual interactions among the particles are taken into account. But this option is often prohibitively time consuming. Thus, our advice is to be very suspicious of results that heavily rely on specific secular resonances. Another implication is that, if the disk is dynamically excited at a specific location (for instance, by a resonance), this excitation does not propagate as a wave through the disk, as it might if the particles' collective effects were correctly modeled (*Ward and Hahn, 1998, 2003*). In turn, this lack of propagation does not damp the excitation at the location where it is triggered. However, wave propagation is possible only if the excitation of the disk is very small [$e < 0.01$, $i < 0.3^{\circ}$ (*Hahn, 2003*)]. Thus, the relevance of this phenomenon remains to be proven in a realistic model of the solar system primordial disk, which is stirred by a number of processes, including the gravitational scattering from a number of Pluto-mass bodies embedded in the disk. In any case, neither of these processes are likely to have a major effect on the planet migration situations discussed in this chapter because the main dynamical driver of migration is relatively close encounters between planets and disk particles. They could have secondary effects, however. For example, if they are active, collective effects could modify the state of the disk particles being fed into the planet-crossing region.

A third limitation is the lack of collisional interaction between the disk particles. At some level, inelastic collisions necessarily damp the dynamical excitation of the disk. However, the importance of this process is a function of many parameters including the surface density of the disk, its dynamical state, and the sizes of individual disk particles. The potential importance of this process was recently pointed out by *Goldreich et al. (2004)*, who considered a case in which the collisional damping is so efficient that any dynamical excitation of the disk due to the planets is almost instantaneously dissipated. Thus, the disk of planetesimals acts as an infinite sink of orbital excitation. *Goldreich et al.* argue that this mechanism can have a huge impact on the process of planet formation and presumably also of planet migration. The disk particle size distribution required for this to happen, however, is rather extreme — essentially all planetesimals need to be ~ 1 cm in diameter.

One of the fundamental issues with the *Goldreich et al.* scenario is whether such an extreme size distribution could actually arise in nature and, if it did, whether it could last long enough to be dynamically important before evolving, either by coagulation (e.g., formation of larger objects) or collisional grinding of itself to dust. However, the existence of both the asteroid and the Kuiper belts suggest that, at

least by the time the planets formed, the planetesimals had a full size distribution ranging up to the sizes of Ceres and Pluto, which, at first glance, seems to be inconsistent with the basic Goldreich et al. scenario. So, although there are many intriguing aspects to this scenario, we believe that it needs to be studied in more detail before its viability can be determined. (The chapter by Chiang et al. presents a new scenario for the formation of the Kuiper belt based on Goldreich et al.'s ideas. However, our ongoing numerical simulations of this scenario have shown that it is not viable, because it leads to a solar system structure that is inconsistent with observations. In particular, we are finding that it leads to planetary systems with too many ice giants, at least one of which is on a nearly circular orbit beyond 30 AU.)

There are published works that will allow us to evaluate whether collisions are important in planetary migration situations when more moderate size distributions are considered. For instance, using a self-consistent planetesimal collision model that includes fragmentation and accretion of debris, *Leinhardt and Richardson (2005)* showed that the runaway growth of planetary embryos is virtually indistinguishable from that obtained in simulations that do not take collisions into account. Considering a realistic size distribution of the disk's planetesimals, *Charnoz and Morbidelli (2003)* showed that the collisional evolution of particles ejected from the Jupiter-Saturn region is moderate, and would affect only a minor portion of the mass. And finally, *Charnoz and Brahic (2001)* studied the process of scattering of planetesimals by a jovian-mass planet taking into account the effect of collisions on the dynamics. They found that Jupiter can still eject particles from its neighborhood and produce a scattered disk of bodies. These results seem to indicate that collisions are probably not important in the overall dynamical evolution of the disk, and consequently on the migration process.

In conclusion, despite the fact that collective effects and collisions are definitely important and must effect, at some level, the evolution of an evolving planetary system, we believe that their role is not significant in the type of planet migration studied in this chapter. Thus, the simulations presented in this chapter should capture the essence of real evolution. We stress that the fact that the simulations presented to support the Nice model reproduce the observed structure of the solar system so well argues that the neglected phenomena only play a secondary role.

9. CLOSING COMMENTS

In this chapter we reviewed the many ways in which massive planetesimal disks can drive changes in the orbits of planets. A planet's orbit can be modified as a result of gravitational encounters with objects from this disk. In particular, if a planet is immersed in a sea of small bodies, it will recoil every time it gravitationally scatters one of these objects. This process allows for the exchange of an-

gular momentum and orbital energy between the planets and the disk. If the disk mass is on the order of the mass of the planets, the planetary orbits can be profoundly modified.

Although there are many ideas in the literature concerning how planetesimal migration could have occurred in the solar system, there is general agreement that it did indeed happen. At the very minimum, the orbital element distribution of objects in the Kuiper belt says that Neptune migrated outward by at least ~ 7 AU (*Malhotra, 1995*). Our understanding of this process in other systems is very limited, however. This is primarily due to the very large number of unknown parameters. However, some of the strange configurations of the extrasolar planetary systems so far discovered could be the result of planetesimal-driven migration. Thus, this field is ripe for further study.

Acknowledgments. H.F.L. thanks NASA's Origins and Planetary Geology and Geophysics programs for supporting his involvement in the research related to this chapter. A.M. is also grateful to CNFA for supporting travel to the Protostars and Planets V conference.

REFERENCES

- Allen R. L., Bernstein G. M., and Malhotra R. (2001a) *Astrophys. J.*, 549, L241–L244.
- Allen R. L., Bernstein G. M., and Malhotra R. (2001b) *Astron. J.*, 124, 2949–2954.
- Backman D. E., Dasgupta A., and Stencel R. E. (1995) *Astrophys. J.*, 405, L35.
- Bernstein G. M., Trilling D. E., Allen R. L., Brown M. E., Holman M., and Malhotra R. (2004) *Astron. J.*, 128, 1364–1390.
- Binney J. and Tremaine S. (1987) *Galactic Dynamics*. Princeton Univ., Princeton.
- Borderies N. and Goldreich P. (1984) *Cel. Mech.*, 32, 127–136.
- Brown M. E. (2001) *Astron. J.*, 121, 2804–2814.
- Chambers J. E. (1999) *Mon. Not. R. Astron. Soc.*, 304, 793–799.
- Chandrasekhar S. (1943) *Astrophys. J.*, 97, 255–262.
- Charnoz S. and Brahic A. (2001) *Astron. Astrophys.*, 375, L31–L34.
- Charnoz S. and Morbidelli A. (2003) *Icarus*, 166, 141–156.
- Chiang E. I. and Brown M. E. (1999) *Astron. J.*, 118, 1411–1422.
- Chiang E. I. and Lithwick Y. (2005) *Astrophys. J.*, 628, 520–532.
- Chiang E. I., Jordan A. B., Millis R. L., Buie M. W., Wasserman L. H., Elliot J. L., Kern S. D., Trilling D. E., Meech K. J., and Wagner R. M. (2003) *Astron. J.*, 126, 430–443.
- Duncan M. J., Levison H. F., and Budd S. M. (1995) *Astron. J.*, 110, 3073–3081.
- Duncan M. J., Levison H. F., and Lee M. H. (1998) *Astron. J.*, 116, 2067–2077.
- Fernandez J. A. and Ip W.-H. (1984) *Icarus*, 58, 109–120.
- Gladman B., Kavelaars J. J., Petit J.-M., Morbidelli A., Holman M. J., and Loredó T. (2001) *Astron. J.*, 122, 1051–1066.
- Goldreich P., Lithwick Y., and Sari R. (2004) *Astrophys. J.*, 614, 497–507.
- Gomes R. S. (1998) *Astron. J.*, 116, 2590–2597.
- Gomes R. S. (2003) *Icarus*, 161, 404–418.
- Gomes R. S., Morbidelli A., and Levison H. F. (GML04) (2004) *Icarus*, 170, 492–507.
- Gomes R., Levison H. F., Tsiganis K., and Morbidelli A. (GLMT05) (2005) *Nature*, 435, 466–469.
- Greaves J. S., Holland W. S., Wyatt M. C., Dent W. R. F., Robson E. I., et al. (2005) *Astrophys. J.*, 619, L187–L190.

- Hahn J. M. (2003) *Astrophys. J.*, 595, 531–549.
- Hahn J. M. and Malhotra R. (1999) *Astron. J.*, 117, 3041–3053.
- Hahn J. M. and Malhotra R. (2005) *Astron. J.*, 130, 2392–2414.
- Hartmann W. K., Ryder G., Dones L., and Grinspoon D. (2000) in *Origin of the Earth and Moon* (R. M. Canup and K. Righter, eds.), pp. 493–512. Univ. of Arizona, Tucson.
- Hayashi C. (1981) In *Fundamental Problems in the Theory of Stellar Evolution* (D. Sugimoto et al., eds.), pp. 113–126. Reidel, Dordrecht.
- Henrard J. (1982) *Cel. Mech.*, 27, 3–22.
- Henrard J. and Lemaître A. (1983) *Icarus*, 55, 482–494.
- Henrard J. and Morbidelli A. (1993) *Phys. D*, 68, 187–200.
- Hollenbach D. and Adams F. C. (2004) In *Debris Disks and the Formation of Planets* (L. Caroff et al., eds.), p. 168. ASP Conf. Series 324, San Francisco.
- Hollenbach D. J., Yorke H. W., and Johnstone D. (2000) In *Protostars and Planets IV* (V. Mannings et al., eds.), p. 401. Univ. of Arizona, Tucson.
- Ida S., Bryden G., Lin D. N. C., and Tanaka H. (IBLT00) (2000) *Astrophys. J.*, 534, 428–445.
- Jewitt D., Luu J., and Chen J. (1996) *Astron. J.*, 112, 1225–1232.
- Jewitt D. C., Trujillo C. A., and Luu J. X. (2000) *Astron. J.*, 120, 1140–1147.
- Kenyon S. J. and Bromley B. C. (2004) *Astron. J.*, 128, 1916–1926.
- Kenyon S. J. and Luu J. X. (1998) *Astron. J.*, 115, 2136–2160.
- Kenyon S. J. and Luu J. X. (1999) *Astron. J.*, 118, 1101–1119.
- Kim J. S., Hines D. C., Backman D. E., Hillenbrand L. A., Meyer M. R., et al. (2005) *Astrophys. J.*, 632, 659.
- Kobayashi H. and Ida S. (2001) *Icarus*, 153, 416–429.
- Leinhardt Z. M. and Richardson D. C. (2005) *Astrophys. J.*, 625, 427–440.
- Levison H. F. and Morbidelli A. (2003) *Nature*, 426, 419–421.
- Levison H. F. and Stern S. A. (2001) *Astron. J.*, 121, 1730–1735.
- Levison H. F. and Stewart G. R. (2001) *Icarus*, 153, 224–228.
- Levison H. F., Lissauer J. J., and Duncan M. J. (1998) *Astron. J.*, 116, 1998–2014.
- Levison H. F., Dones L., Chapman C. R., Stern S. A., Duncan M. J., and Zahnle K. (2001) *Icarus*, 151, 286–306.
- Levison H. F., Morbidelli A., and Dones L. (2004) *Astron. J.*, 128, 2553–2563.
- Malhotra R. (1993) *Nature*, 365, 819–821.
- Malhotra R. (1995) *Astron. J.*, 110, 420–429.
- Michtchenko T. A., Beaugé C., and Roig F. (2001) *Astron. J.*, 122, 3485–3491.
- Morbidelli A., Brown M. E., and Levison H. F. (2003) *Earth Moon Planets*, 92, 1–27.
- Morbidelli A., Levison H. F., Tsiganis K., and Gomes R. (MLTG05) (2005a) *Nature*, 435, 462–465.
- Morbidelli A., Crida A., and Masset F. (2005b) *AAS/DPS Meeting #37*, Abstract #25.07.
- Moorhead A. V. and Adams F. C. (2005) *Icarus*, 178, 517–539.
- Murray N., Hansen B., Holman M., and Tremaine S. (1998) *Science*, 279, 69.
- Murray-Clay R. A. and Chiang E. I. (2005) *Astrophys. J.*, 619, 623–638.
- Neishtadt A. I. (1975) *J. Appl. Math. Mech.*, 39, 594–605.
- Neishtadt A. I. (1987) *Prikl. Mat. Mek.*, 51, 750–757.
- Neishtadt A. I. (1997) *Cel. Mech.*, 65, 1–20.
- O'Brien D. P., Morbidelli A., and Bottke W. F. (2005) *AAS/DPS Meeting #37*, Abstract #29.14.
- Opik E. J. (1976) *Interplanetary Encounters: Close-Range Gravitational Interactions*. Elsevier, Amsterdam.
- Ozernoy L. M., Gorkavyi N. N., Mather J. C., and Taidakova T. A. (2000) *Astrophys. J.*, 537, L147–L151.
- Papaloizou J. C. B. and Terquem C. (2001) *Mon. Not. R. Astron. Soc.*, 325, 221–230.
- Papaloizou J. C. B. and Terquem C. (2006) *Rep. Prog. Phys.*, 69, 119–180.
- Petit J.-M. and Mousis O. (2004) *Icarus*, 168, 409–419.
- Podosek F. A. and Cassen P. (1994) *Meteoritics*, 29, 6–55.
- Pollack J. B., Hubickyj O., Bodenheimer P., Lissauer J. J., Podolak M., and Greenzweig Y. (1996) *Icarus*, 124, 62–85.
- Rasio F. A. and Ford A. B. (1996) *Science*, 274, 954–956.
- Rieke G. H., Su K. Y. L., Stansberry J. A., Trilling D., Bryden G., Muzerolle J., White B., Gorlova N., Young E. T., Beichman C. A., Stapelfeldt K. R., and Hines D. C. (2005) *Astrophys. J.*, 620, 1010–1026.
- Schneider J. (2004) *Extra Solar Planets Encyclopaedia*, vo.obspm.fr/exoplanetes/encyclo/encycl.html.
- Stern S. A. (1996) *Astron. J.*, 112, 1203–1211.
- Stern S. A. and Colwell J. E. (1997a) *Astron. J.*, 112, 841–849.
- Stern S. A. and Colwell J. E. (1997b) *Astrophys. J.*, 490, 879–885.
- Stone J. M., Ostriker E. C., and Gammie C. F. (1998) *Astrophys. J.*, 508, L99–L102.
- Tegler S. C. and Romanishin W. (2003) *Icarus*, 161, 181–191.
- Tera F., Papanastassiou D. A., and Wasserburg G. J. (1974) *Earth Planet. Sci.*, 22, L1–21.
- Thi W. F., Blake G. A., van Dishoeck E. F., van Zadelhoff G. J., Horn J. M. M., Becklin E. E., Mannings V., Sargent A. I., Van den Ancker M. E., and Natta A. (2001) *Nature*, 409, 60–63.
- Thommes E. W., Duncan M. J., and Levison H. F. (1999) *Nature*, 402, 635–638.
- Trujillo C. A. and Brown M. E. (2001) *Astrophys. J.*, 554, L95–L98.
- Trujillo C. A. and Brown M. E. (2002) *Astrophys. J.*, 566, 125–128.
- Trujillo C. A., Jewitt D. C., and Luu J. X. (2001) *Astron. J.*, 122, 457–473.
- Tsiganis K., Gomes R., Morbidelli A., and Levison H. F. (TGML05) (2005) *Nature*, 435, 459–461.
- Valsecchi A. and Manara G. B. (1997) *Astron. Astrophys.*, 323, 986–998.
- Wahhaj Z., Koerner D. W., Ressler M. E., Werner M. W., Backman D. E., and Sargent A. I. (2003) *Astrophys. J.*, 584, L27–L31.
- Ward W. R. and Hahn J. M. (1998) *Astron. J.*, 116, 489–498.
- Ward W. R. and Hahn J. M. (2003) *Astron. J.*, 125, 3389–3397.
- Weidenschilling S. J. (2003) *Icarus*, 165, 438–442.
- Weidenschilling S. J. and Marzari F. (1996) *Nature*, 384, 619–621.
- Wiggins S. (1991) *Chaotic Transport in Dynamical Systems*. Springer-Verlag, New York.
- Wyatt M. C. (2003) *Astrophys. J.*, 598, 1321–1340.
- Wyatt M. C. (2005) *Astron. Astrophys.*, 440, 937–948.
- Wyatt M. C., Greaves J. S., Dent W. R. F., and Coulson I. M. (2005) *Astrophys. J.*, 620, 492–500.
- Yoshida F. and Nakamura T. (2005) *Astron. J.*, 130, 2900–2911.
- Youldin A. N. and Shu F. H. (2002) *Astrophys. J.*, 580, 494–505.